Lect4. Holographic study of strongly interacting QCD matter under extreme conditions

侯德富

华中师范大学粒子物理研究所

Outlines

- Introduction and motivation
- Phase structure under rotation and Magnetic field
- Transport properties rotating magnetized matter
- Summary

QCD under new extreme conditions

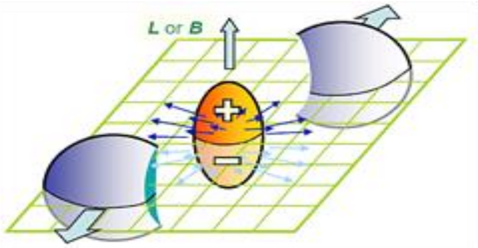

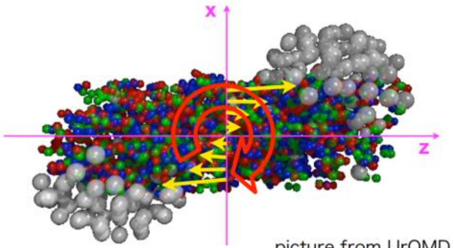

picture from UrQMD

$$E, B \sim \gamma \frac{Z\alpha_{EM}}{R_A^2} \sim 3m_\pi^2$$

$$L \approx \frac{A\sqrt{s_{NN}}}{2} b\hbar \sim 10^6\hbar$$

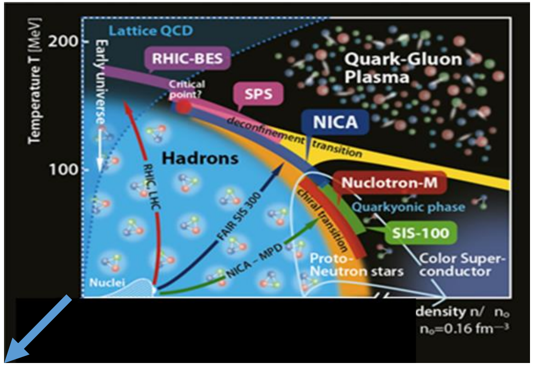

B, ω

Explore the new dimensions of the QCD phase diagram

Khazeev, Liao Nature 2021, Becattini- Karpenko etal 2015, 2016; Jiang-Lin-Liao 2016; Deng-XGH-Ma-Zhang 2020; Deng-XGH 2016, Xie-Csernai etal 2014; Pang-Petersen-Wang-Wang 2016; Xia-Li-Wang 2017,2018; Sun-Ko 2017;… …)

AdS/CFT

AdS/CFT correspondence (holography), the duality between the string theory in AdS bulk and N = 4 SYM theory on the boundary*.

AdS/CFT can be seen as a concrete implementation of the holographic principle.

*Juan Martin Maldacena. Int.J.Theor.Phys. 38 (1999) 1113-1133, Adv.Theor.Math.Phys. 2 (1998) 231-252. (17624 citations)

*Edward Witten. Adv.Theor.Math.Phys. 2 (1998) 253-291. (11301 citations)

*S.S. Gubser, Igor R. Klebanov, Alexander M. Polyakov. Phys.Lett.B 428 (1998) 105-114.(9525 citations)

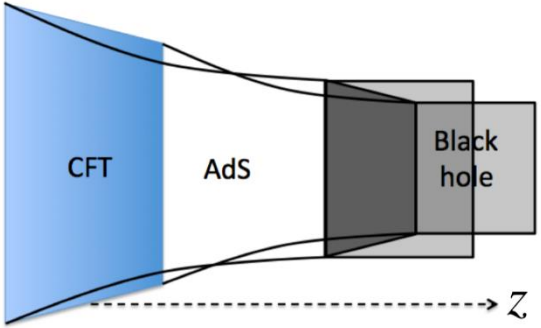

$$\mathrm{N} = 4\ \mathrm{SYM\ on\ the\ boundary} \quad \Leftrightarrow \quad \mathrm{Type\ IIB\ string\ theory\ in\ the\ bulk}$$

$$\mathrm{conformal\ group\ in\ CFT} \quad = \quad \mathrm{isometry\ group\ in\ AdS}$$

$$\mathrm{partition\ function:} \quad Z_{\mathrm{SYM}} \quad = \quad Z_{\mathrm{string}}$$

$$\lambda \equiv N_c g_{\mathrm{YM}}^2 \quad = \quad \frac{1}{\alpha'^2} \qquad (\mathrm{string\ tension} = \frac{1}{2\pi\alpha'})$$

$$\frac{\lambda}{N_c} \quad = \quad 4\pi g_s$$

The AdS/CFT duality spans all physics arXivs

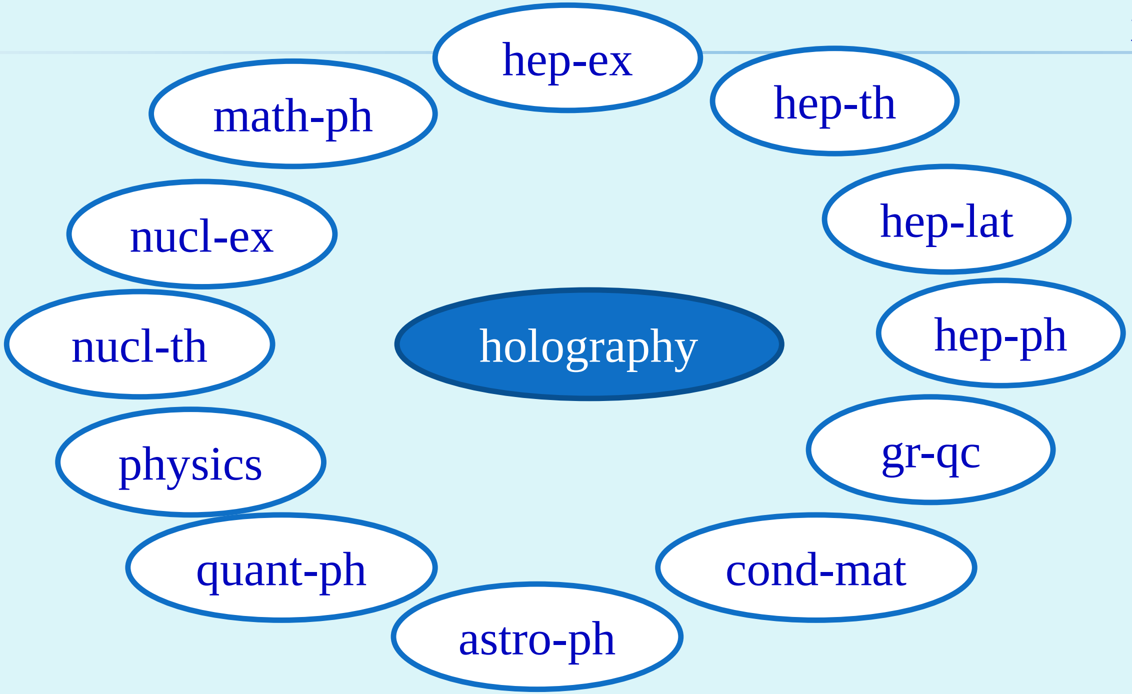

hep-ph*:
black hole thermodynamics,
energy loss,
QCD phase diagram,
etc.

Phase Structure of hQCD with magnetic field

The Einstein-Maxwell-dilaton(EMD) action *:

$$S=-\frac{1}{16\pi G_5}\int d^5x\sqrt{-g}[R-\frac{f_1(\phi)}{4}F_{(1)MN}F^{MN}-\frac{f_2(\phi)}{4}F_{(2)MN}F^{MN}-\frac{1}{2}\partial_M\phi\partial^M\phi-V(\phi)],$$

chemical potential　B field　breaking conformal sym.

The metric:

$$ds^2=\frac{L^2e^{S(z)}}{z^2}[-g(z)dt^2+dx_1^2+e^{B^2z^2}(dx_2^2+dx_3^2)+\frac{dz^2}{g(z)}],$$

$$A_t(z)=\mu[1-\frac{\int_0^z d\xi\frac{\xi e^{-B^2\xi^2}}{f_1(\xi)\sqrt{S(\xi)}}}{\int_0^{z_h} d\xi\frac{\xi e^{-B^2\xi^2}}{f_1(\xi)\sqrt{S(\xi)}}}]=\widetilde{\mu}\int_z^{z_h}d\xi\frac{\xi e^{-B^2\xi^2}}{f_1(\xi)\sqrt{S(\xi)}},$$

Dilaton field :

$$\phi(z)=\int dz\sqrt{-\frac{2}{z}(3zA''(z)-3zA'(z)^2+6A'(z)+2B^4z^3+2B^2z)}+K_5.$$

*Hardik Bohra a, David Dudal et al, Anisotropic string tensions and IMC from a dynamical AdS/QCD model.PLB 801 (2020) 135184.

BH thermodynamics of hot dense hQCD

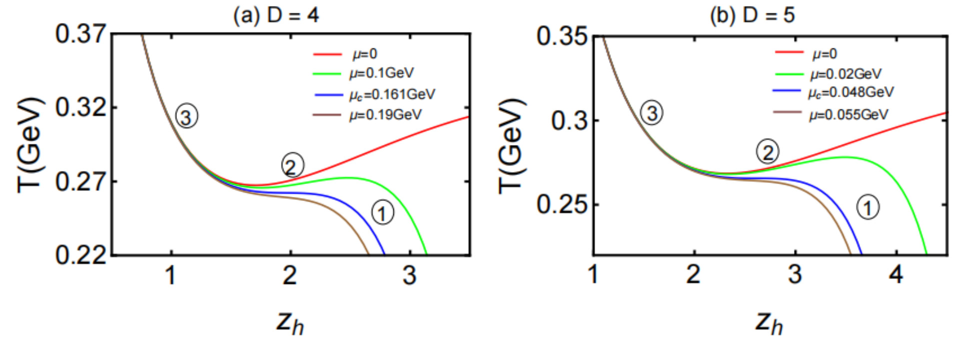

图16. D维下温度跟视界关系

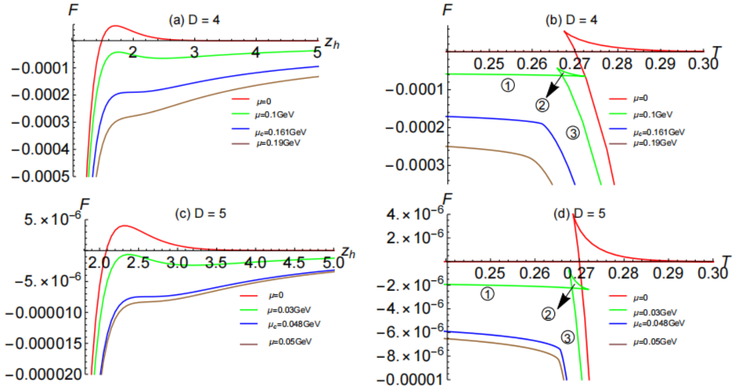

图17. D维下的自由能

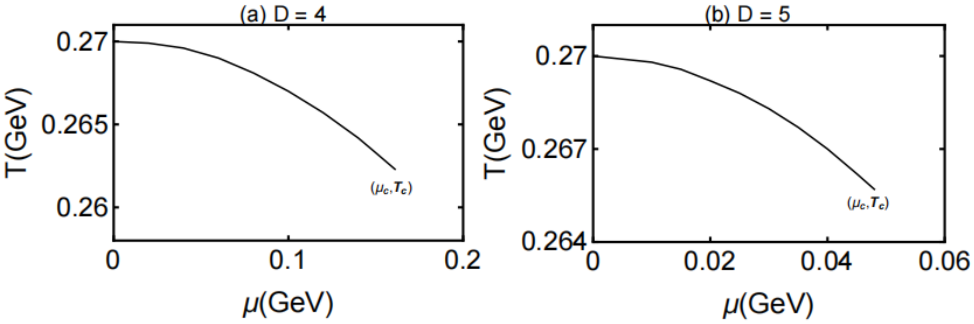

图18. D维下相图

1）一阶相变附近温度、自由能非单调；平滑过渡附近单调；
2）维度较低时，临界μ_{CEP}更大

Zhou-Run Zhu, Jun-Xia Chen, Xian-Ming Liu, De-fu Hou, **Eur.Phys.J.C 82 (2022) 6,560.**

BH thermodynamics and hQCD PT with B

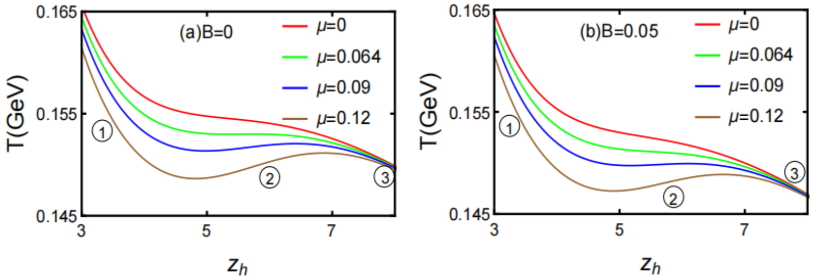

图1. 化学势对温度的影响

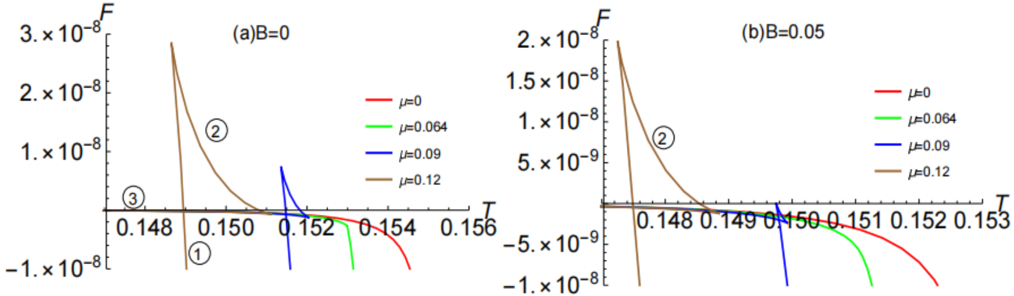

图2. 化学势对吉布斯自由能的影响

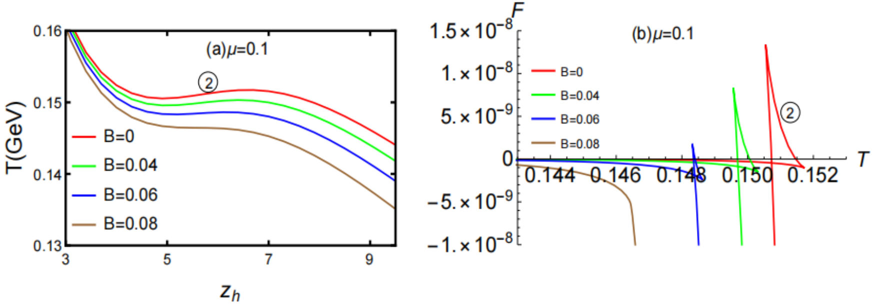

图3. 磁场对温度、自由能的影响

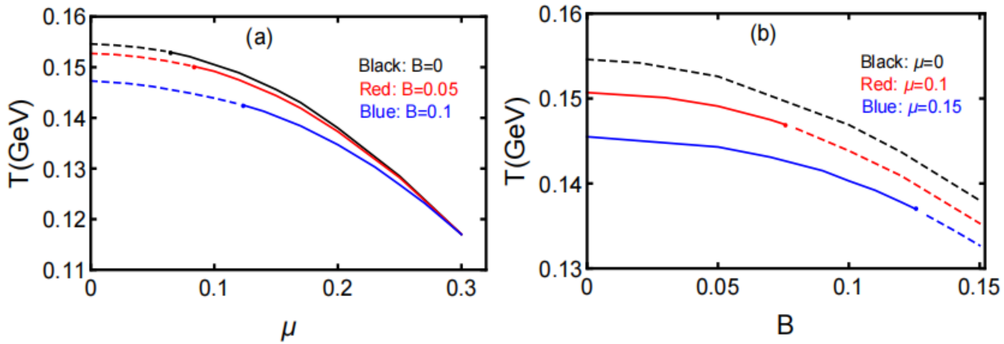

图4. 相图

1）μ促使相变从平滑过渡转变为一阶；B促使相变从一阶转变为平滑过渡；

2）反磁催化；B增大了临界μ_{CEP}，化学势增大了临界B_{CEP}。

Zhou-Run Zhu, De-fu Hou, Inverse magnetic catalysis and energy loss in holographic QCD model, (arXiv:2305.12375), will appear in PRD (2024).

Phase Structure with magnetic field

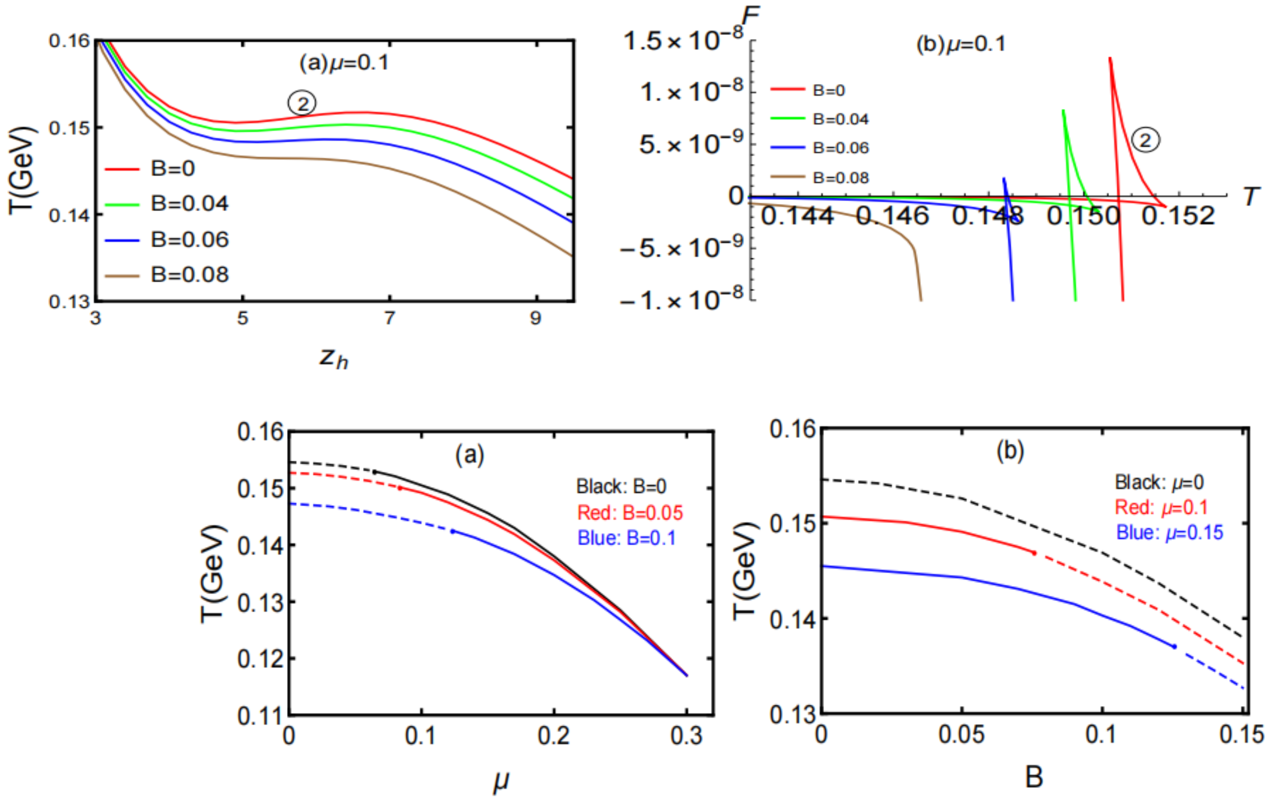

Zhou-Run Zhu, De-fu Hou, (arXiv:2305.12375), will appear PRD (2024)

Phase diagram @2+1 flavor

➢ **Holographic model:**

[1] R.G. Cai, etc , Phys.Rev.D 106 (2022) 12, L121902 • e-Print: 2201.02004

➢ **The action:**

$$S_M = \frac{1}{2\kappa_N^2}\int d^5x\sqrt{-g}[\mathcal{R} - \frac{1}{2}\nabla_\mu\phi\nabla^\mu\phi - \frac{Z(\phi)}{4}F_{\mu\nu}F^{\mu\nu} - V(\phi)],$$

where the potential and kinetic functions read

$$V(\phi) = -12\cosh[c_1\phi] + \left(6c_1^2 - \frac{3}{2}\right)\phi^2 + c_2\phi^6,$$

Capturing the behavior of EOS at zero chemical potential.

$$Z(\phi) = \frac{1}{1+c_3}\mathrm{sech}[c_4\phi^3] + \frac{c_3}{1+c_3}e^{-c_5\phi}.$$

Capturing the flavor dynamic.

➢ **The metric:**

$$ds^2 = -e^{-\eta(r)}f(r)dt^2 + \frac{dr^2}{f(r)} + r^2(dx_1^2 + dx_2^2 + dx_3^2),$$

$$\phi = \phi(r), \qquad A_t = A_t(r),$$

➢ **The Hawking temperature and entropy density:**

$$T = \frac{1}{4\pi}f'(r_h)e^{-\eta(r_h)/2} \qquad s = \frac{2\pi}{\kappa_N^2}r_h^3.$$

effective Newton constant

➢ The parameter:

model	c_1	c_2	c_3	c_4	c_5	κ_N^2	ϕ_s(GeV)	b
pure $SU(3)$	0.735	0				$2\pi(4.88)$	1.523	-0.36458
2 flavor	0.710	0.0002	0.530	0.085	30	$2\pi(3.72)$	1.227	-0.25707
2+1 flavor	0.710	0.0037	1.935	0.085	30	$2\pi(1.68)$	1.085	-0.27341

[5]. S. He, L. Li, Z. Li and S. Wang, [arXiv:2210.14094]

[2]. Y.-Q. Zhao, S. He, D. Hou, L. Li and Z. Li, , [2310.13432].

[1]. R.-G. Cai, S. He, L. Li and Y.-X. Wang, Phys. Rev. D 106 (2022) L121902 [arXiv:2201.02004]

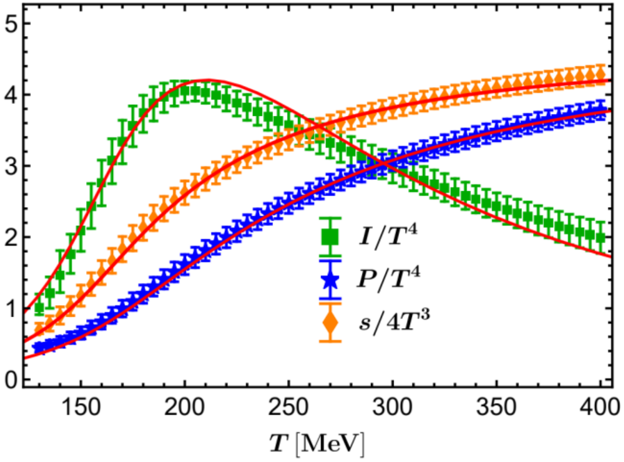

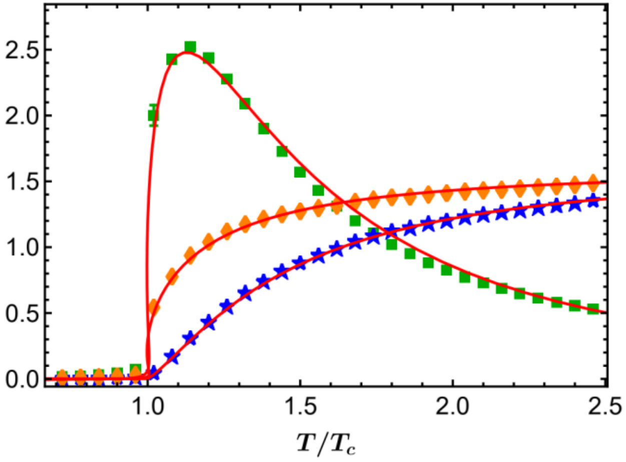

Lattice

[3]. Phys.Rev.D 90 (2014) 094503
•e-Print: 1407.6387

[4]. Phys.Rev.D 98 (2018) 5, 054513
• e-Print: 1801.03110

Phase diagram @2+1 flavor

- **Holographic model *with rotation*:**
  - **To introduce the rotation effect, we split the 3-dimensional space into two parts as** $\mathcal{M}_3 = \mathbb{R} \times \Sigma_2$. **Then the metric becomes to**

$$\boxed{ds^2 = -f(r)e^{-\eta(r)}dt^2 + \frac{dr^2}{f(r)} + r^2\ell^2 d\theta^2 + r^2 d\sigma^2}$$

where $d\sigma^2$ denotes the line element of Σ_2.

  - **We assume the system that has an angular velocity ω with a fixed radius ℓ, and consider the following local Lorentz boost**

[5]. JHEP 07 (2021) 132 • e-Print: 2010.14478 [6].Phys.Rev.D 97 (2018) 2, 024034 • e-Print: 1707.03483
[7].JHEP 04 (2017) 092 • e-Print: 1702.02416 [8].Gen.Rel.Grav. 42 (2010) 1571-1583 • e-Print: 0911.2831

$$\boxed{t \to \frac{1}{\sqrt{1-\omega^2\ell^2}}(\hat{t} + \omega\ell^2\hat{\theta}), \qquad \theta \to \frac{1}{\sqrt{1-\omega^2\ell^2}}(\hat{\theta} + \omega\hat{t})}\,.$$

  - **The corresponding metric can be written as**

$$\boxed{d\hat{s}^2 = g_{\mu\nu}d\hat{x}^\mu d\hat{x}^\nu = -N(r)d\hat{t}^2 + \frac{dr^2}{f(r)} + R(r)(d\hat{\theta} + Q(r)d\hat{t})^2 + r^2 d\sigma^2}\,,$$

$$N(r) = \frac{r^2 f(r)\left(1-\omega^2\ell^2\right)}{r^2 e^{\eta(r)} - \omega^2\ell^2 f(r)}\,,$$

$$R(r) = \frac{r^2\ell^2 - \omega^2\ell^4 f(r)e^{-\eta(r)}}{1-\omega^2\ell^2}\,,$$

$$Q(r) = \frac{\omega\left(f(r) - r^2 e^{\eta(r)}\right)}{\omega^2\ell^2 f(r) - r^2 e^{\eta(r)}}\,.$$

Phase diagram @2+1 flavor

➤ Holographic model:

[1] R.G. Cai, etc , Phys.Rev.D 106 (2022) 12, L121902 • e-Print: 2201.02004

➤ **The action:**

$$\boxed{S_M = \frac{1}{2\kappa_N^2}\int d^5x\sqrt{-g}[\mathcal{R} - \frac{1}{2}\nabla_\mu\phi\nabla^\mu\phi - \frac{Z(\phi)}{4}F_{\mu\nu}F^{\mu\nu} - V(\phi)]\,,}$$

where the potential and kinetic functions read

$$V(\phi) = -12\cosh\left[c_1\phi\right] + \left(6c_1^2 - \frac{3}{2}\right)\phi^2 + c_2\phi^6,$$

Capturing the behavior of EOS at zero chemical potential.

$$Z(\phi) = \frac{1}{1+c_3}\mathrm{sech}[c_4\phi^3] + \frac{c_3}{1+c_3}e^{-c_5\phi}.$$

Capturing the flavor dynamic.

➤ **The metric:**

$$ds^2 = -e^{-\eta(r)}f(r)dt^2 + \frac{dr^2}{f(r)} + r^2(dx_1^2 + dx_2^2 + dx_3^2),$$

$$\phi = \phi(r), \qquad A_t = A_t(r),$$

➤ **The Hawking temperature and entropy density:**

$$T = \frac{1}{4\pi}f'(r_h)e^{-\eta(r_h)/2} \qquad s = \frac{2\pi}{\kappa_N^2}r_h^3.$$

effective Newton constant

Phase diagram @2+1 flavor

- **Thermodynamics *with rotation*:**

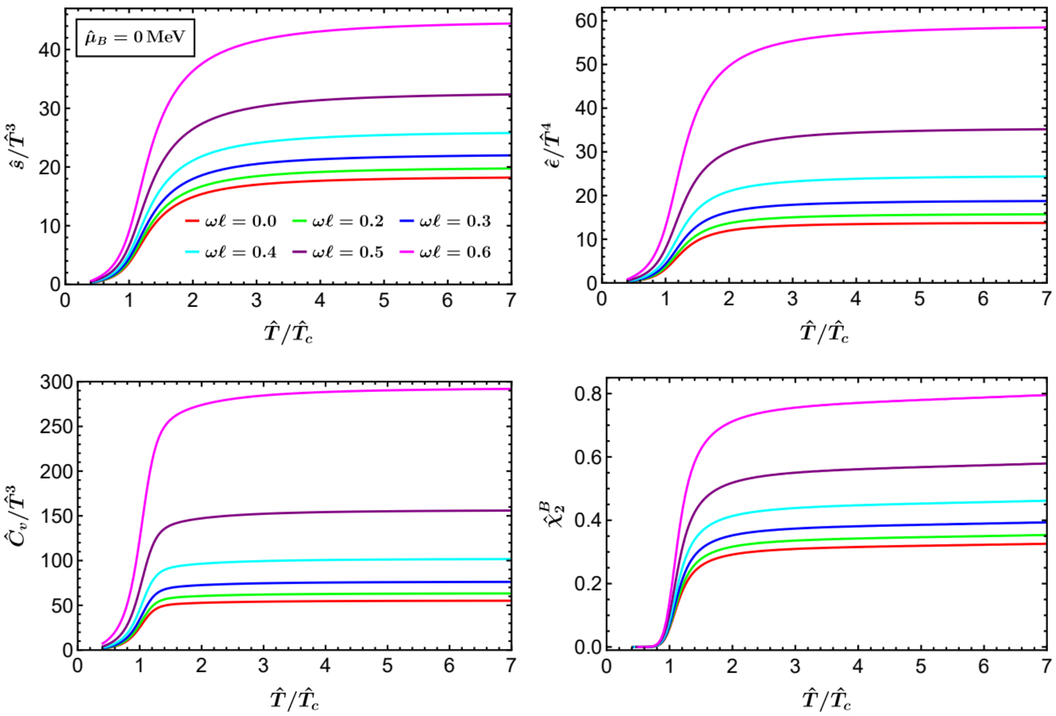

Yan-Qing Zhao, Song He, Defu Hou, Li Li, Zhibin Li, JHEP 04 (2023) 115 • e-Print: 2212.14662

➤ Thermodynamics *with rotation*:

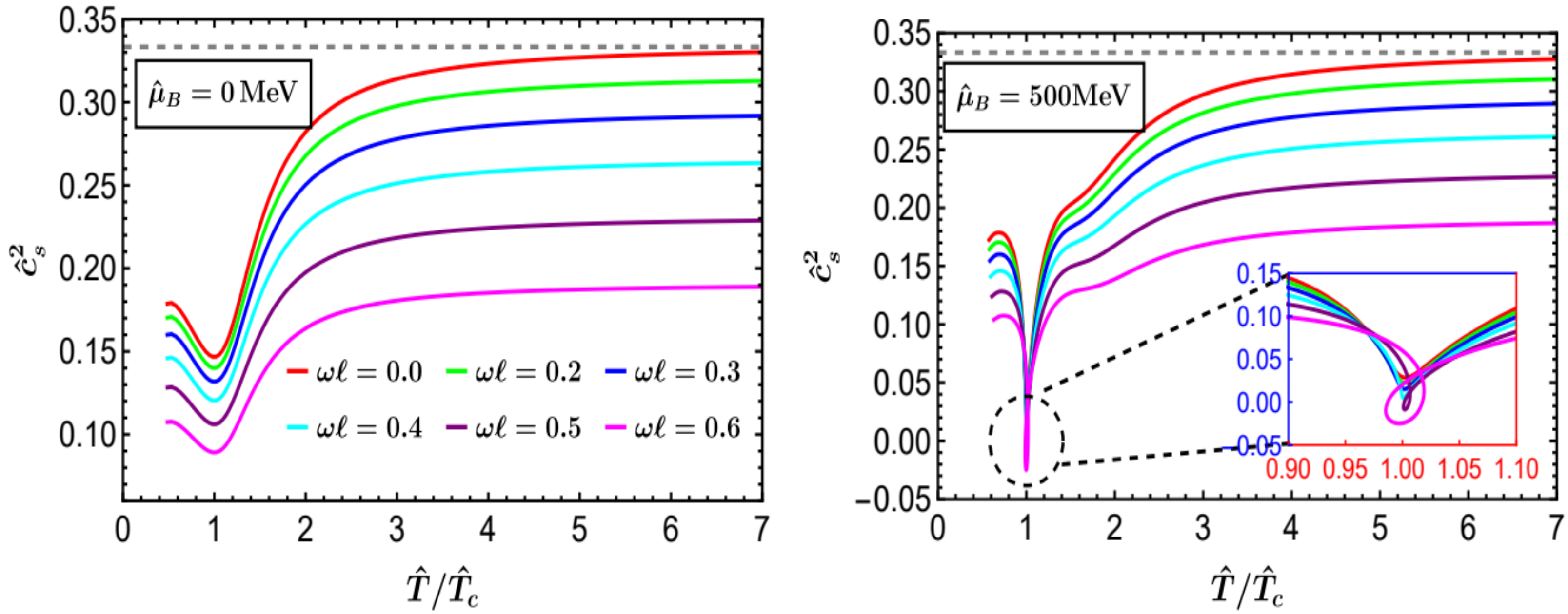

Yan-Qing Zhao, Song He, Defu Hou, Li Li, Zhibin Li, JHEP 04 (2023) 115 • e-Print: 2212.14662

ID: *Yan-Qing Zhao, Song He, Defu Hou, Li Li, Zhibin Li, JHEP 04 (2023) 115 • e-Print: 2212.14662*

➢ 2+1 flavor:

➢ Pure gluon($\hat{\mu}_B = 0$):

- ✓ **black solid line:** denoting the location of CEP.
- ✓ At high $\hat{T}$and small $\hat{\mu}_B$: **Being the smooth crossover.**
- ✓ At low $\hat{T}$and large $\hat{\mu}_B$: **Being 1st-order transition.**
- ✓ $\omega \uparrow$ ⟹ $\hat{T}_c \downarrow$, $\hat{\mu}_c \downarrow$, $\hat{T}_{cep} \downarrow$, $\hat{\mu}_{cep} \downarrow$.

Analytically: $\hat{T}_c(\omega) = T_c\sqrt{1-\omega^2\ell^2}$

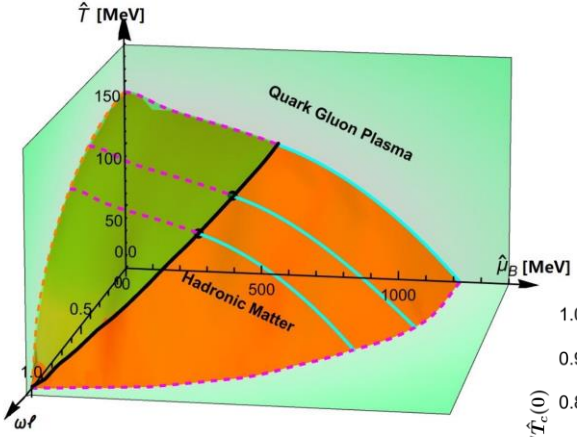

$$\hat{T}_c(\omega)/\hat{T}_c(0) \approx 1 - c\,\omega^2$$

- ✓ At finite $\hat{\mu}_B$ **and smaller ω.**

  The value of c depends on $\hat{\mu}_B$.

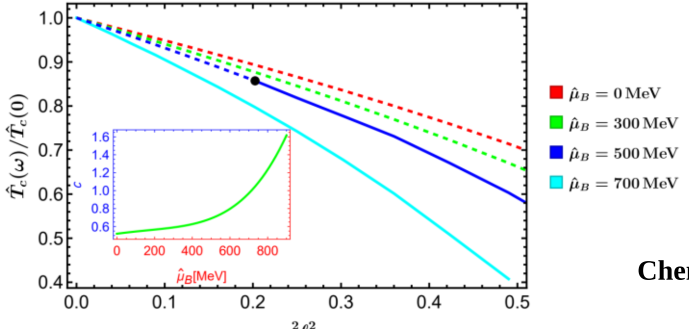

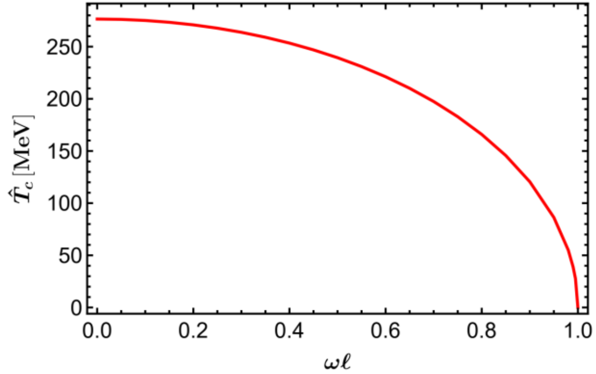

Chen, Zhang, Li, Hou , M.Huang ,JHEP 07 (2021) 132

Phase structure and critical phenomena in 2-flavor QCD

Yan-Qing Zhao, Song He, Defu Hou, Li Li, Zhibin Li （ Phys.Rev.D 109 (2024) 8, 086015 ）

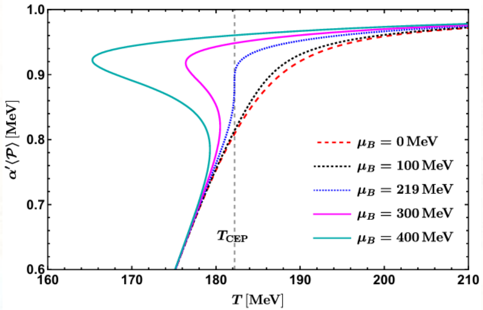

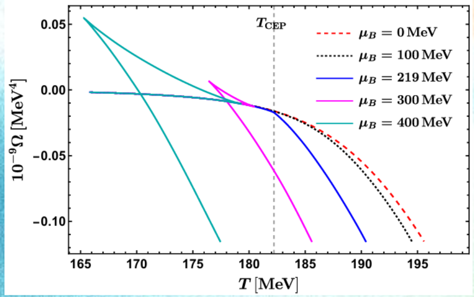

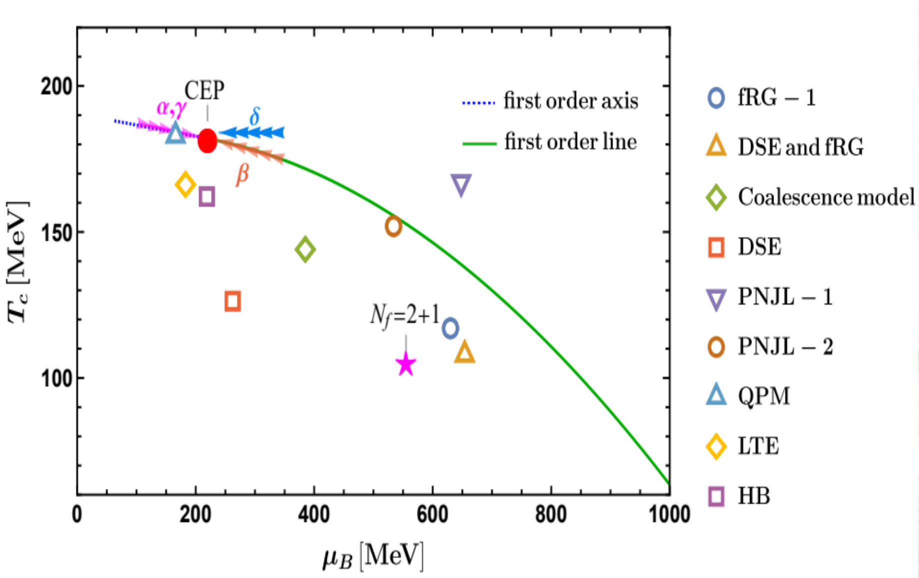

Yan-Qing Zhao, Song He, Defu Hou, Li Li, Zhibin Li （ Phys.Rev.D 109 (2024) 8, 086015 ）

临界现象:

$$C_n \equiv T\left(\frac{\partial s}{\partial T}\right)_{n_B} \sim |T - T_{\text{CEP}}|^{-\alpha}$$

$$\Delta s = s_> - s_< \sim (T_{\text{CEP}} - T)^{\beta}.$$

$$\chi_2^B = \frac{1}{T^2}\left(\frac{\partial n_B}{\partial \mu_B}\right)_T \sim |T - T_{\text{CEP}}|^{-\gamma}.$$

$$s - s_{\text{CEP}} \sim \left|\mu_B - \mu_{\text{CEP}}\right|^{1/\delta}$$

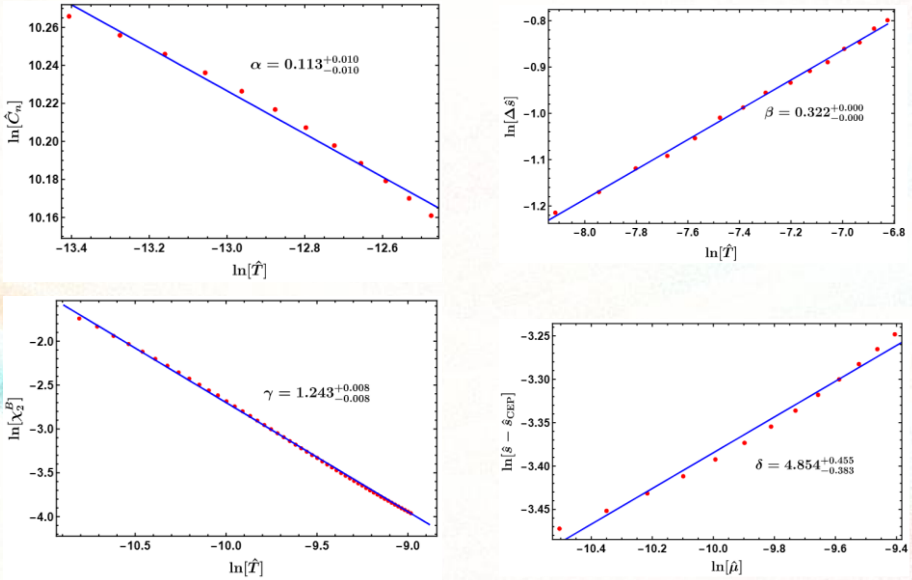

Phase structure and critical phenomena in two-flavor QCD by holography（Phys.Rev.D 109 (2024) 8, 086015）

Yan-Qing Zhao, Song He, Defu Hou, Li Li, Zhibin Li

$\boxed{\text{标度关系:}}$ $\alpha + 2\beta + \gamma = 2, \quad \alpha + \beta(1+\delta) = 2\,.$

	Experiment	3D Ising	Mean field	DGR model	Ours
α	0.110-0.116	0.110(5)	0	0	$0.113^{+0.010}_{-0.010}$
β	0.316-0.327	0.325±0.0015	1/2	0.482	$0.322^{+0.000}_{-0.000}$
γ	1.23-1.25	1.2405±0.0015	1	0.942	$1.243^{+0.008}_{-0.008}$
δ	4.6-4.9	4.82(4)	3	3.035	$4.854^{+0.455}_{-0.383}$

[3]O. DeWolfe, S.S. Gubser and C. Rosen, A holographic critical point, Phys. Rev. D 83 (2011) 086005 [1012.1864].

[4]N. Goldenfeld, Lectures on phase transitions and the renormalization group (1992).

Gravitational waves from holographic QCD phase transition .

Zhou-Run Zhu, Jun Chen, Defu Hou. Eur.Phys.J.A 58 (2022) 6, 104

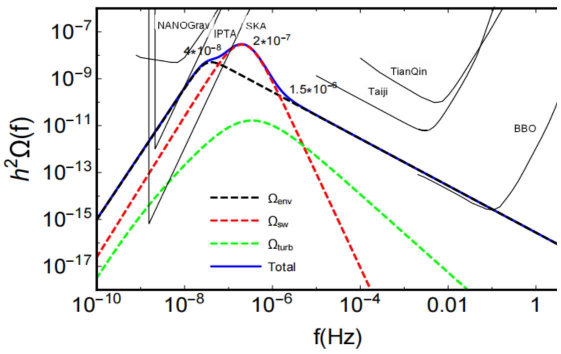

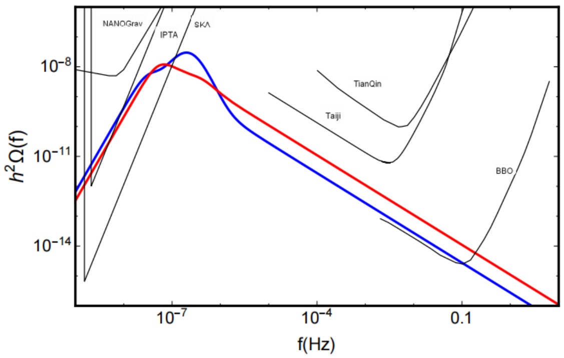

结论：峰值频率是由声波决定；胶子凝聚抑制了总引力波的能量密度和峰值频率。

The spectral function of heavy vector mesons

Mamani , Hou, Braga, PRD 105, 126020 (2022)

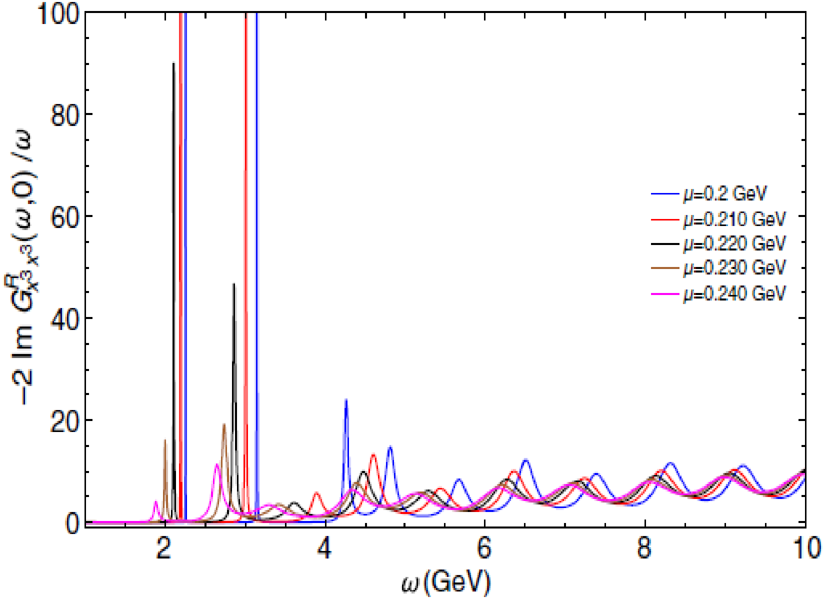

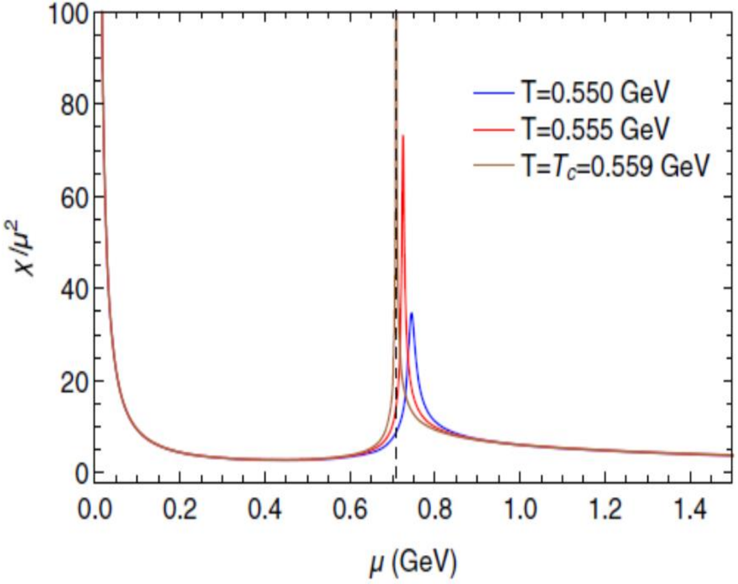

J/Ψ

- **Spectral function:**

Yan-Qing Zhao, Defu Hou, Eur.Phys.J.C 82 (2022) 12, 1102 • e-Print: 2108.08479

As increasing magnetic field, the dissociation effect increases and it is stronger for the parallel case.

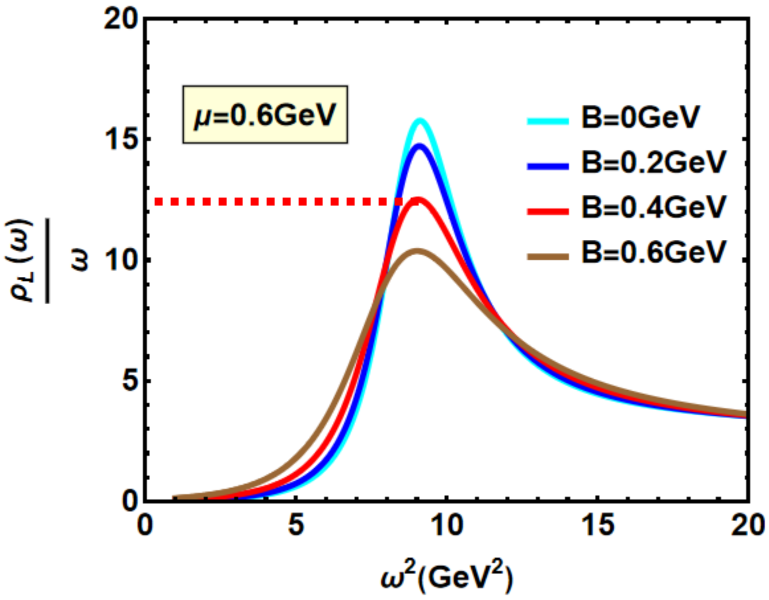

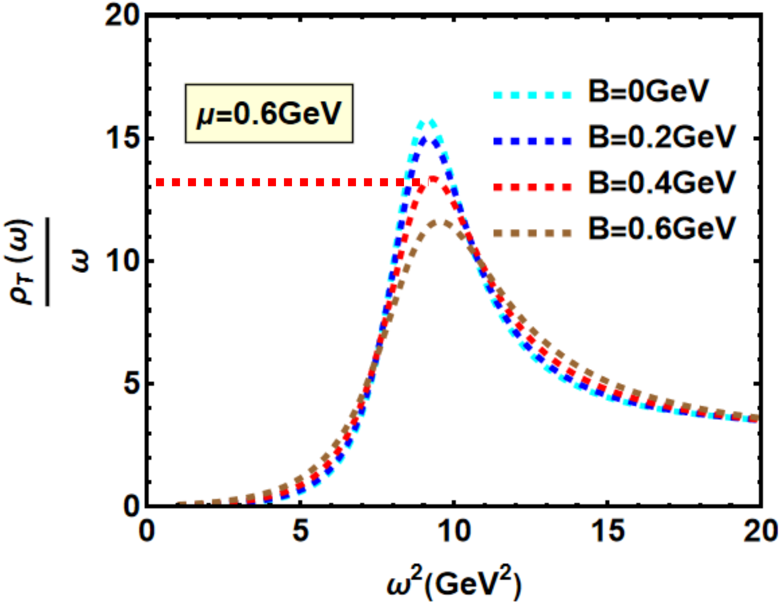

J/Ψ 和 ϒ(1S) 的谱函数

W.B. Chang and De-Fu Hou, Phys. Rev. D 109, 086010 (2024).

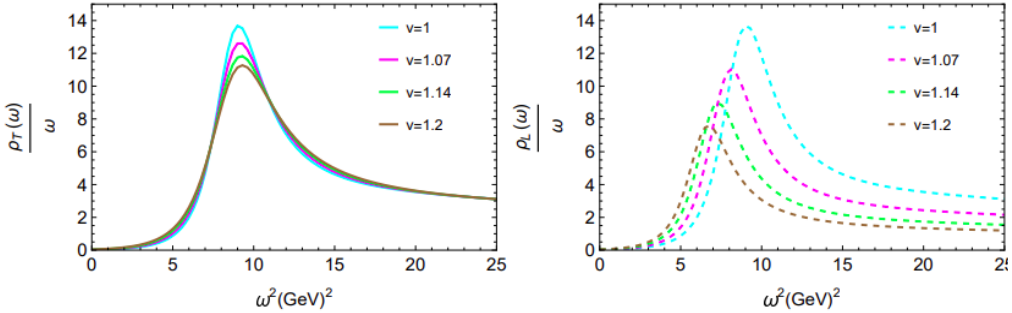

图4. 不同的各向异性参数下，J/Ψ 的谱函数

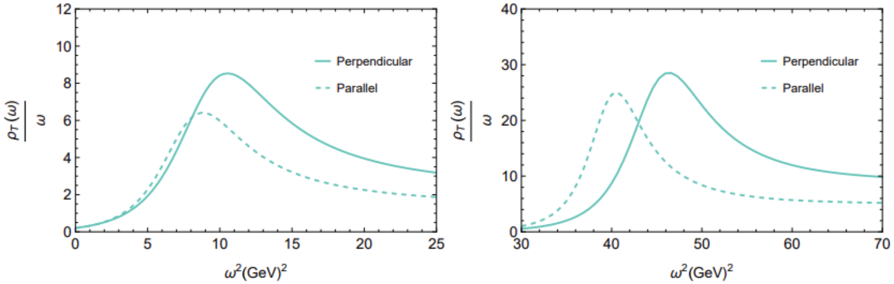

图6. 实线代表各向异性与极化方向垂直
虚线代表各向异性与极化方向平行

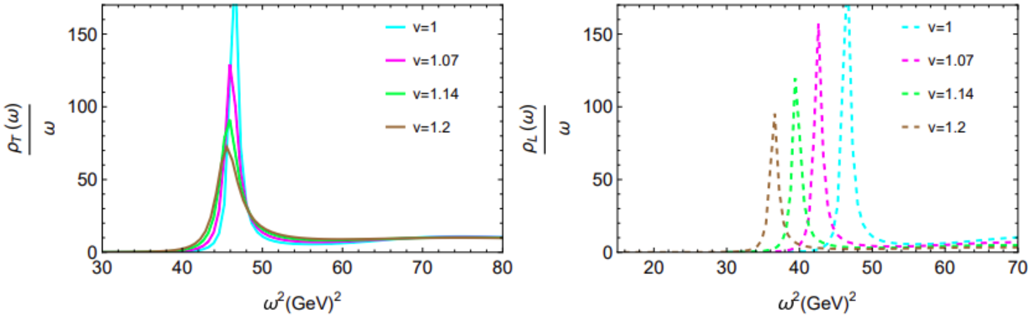

图5. 不同的各向异性参数下，ϒ(1S) 的谱函数

1） 各向异性会加速束缚态的溶解
2） 各向异性方向与极化方向平行时，这一其效应更为显著

J/Ψ 和 ϒ(1S) 的谱函数

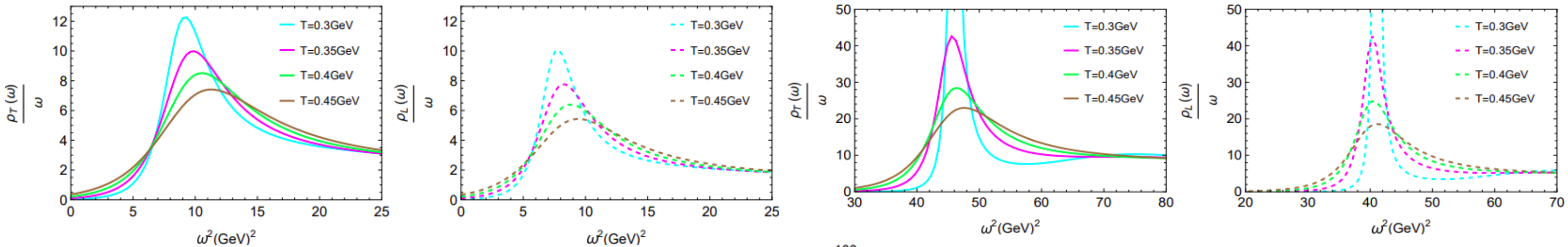

图7. 温度

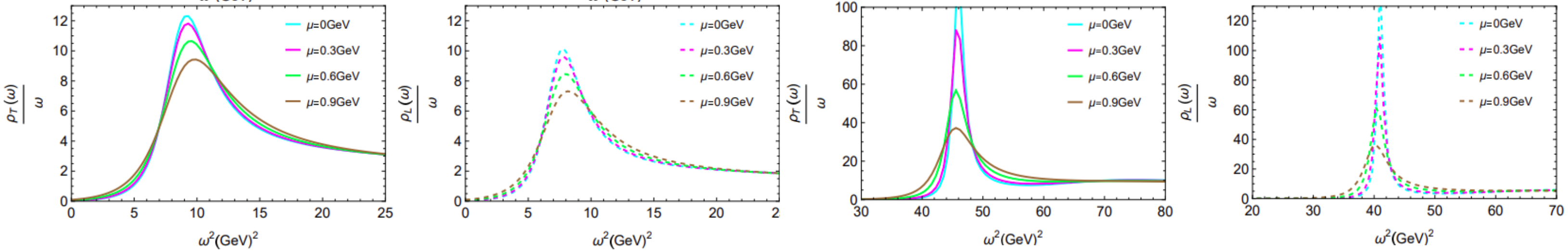

图8. 化学势

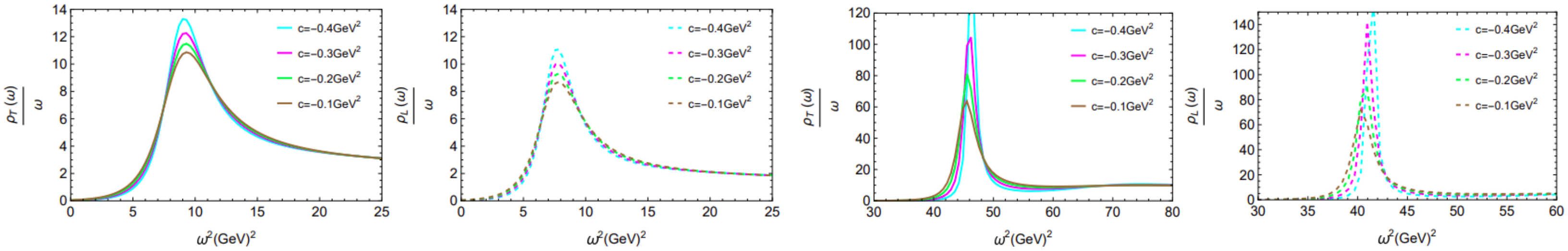

图9. 弯曲因子

3) 有限温度和密度效应会导致重夸克偶素的熔解
4) 更大的弯曲因子会增强溶解效应

W.B. Chang and DH, Phys. Rev. D 109, 086010 (2024).

Jet quenching in QGP

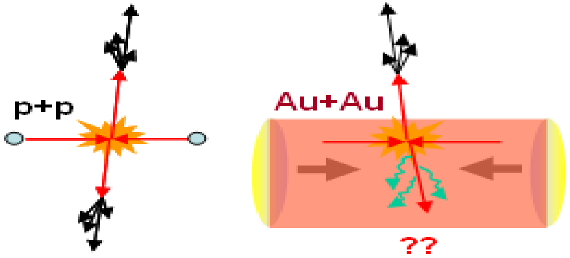

$$\Delta E \approx -\frac{\alpha_S}{2\pi} N_C \, \hat{q} \, L^2$$

Baier, Dokshitzer, Mueller,Peigne, Schiff (1996):

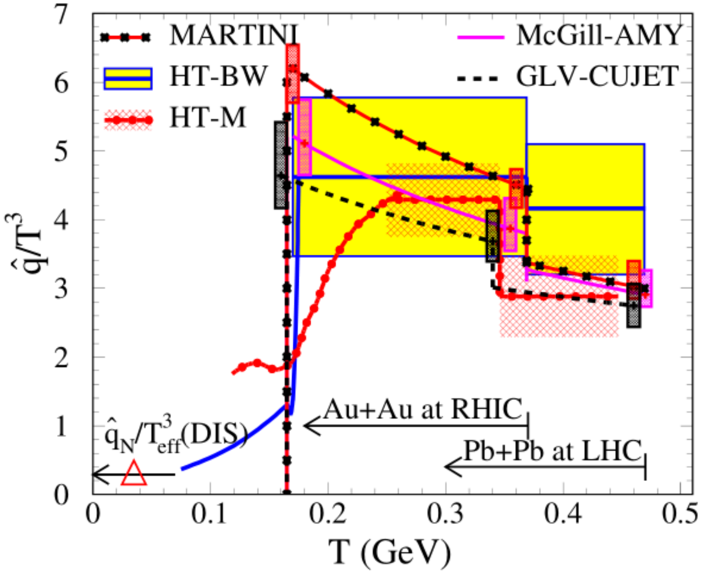

Jet Collaboration, PRC 90,014909(2014)

Energy loss and jet quenching

$$\langle W^A[C]\rangle \approx exp(-\frac{1}{4\sqrt{2}}\hat{q}L_-L^2) \quad \langle W^F[C]\rangle \approx exp[-S_I]$$

$$\hat{q}_0 = \frac{\pi^{3/2}\Gamma(\frac{3}{4})}{\Gamma(\frac{5}{4})}\sqrt{\lambda}T^3$$

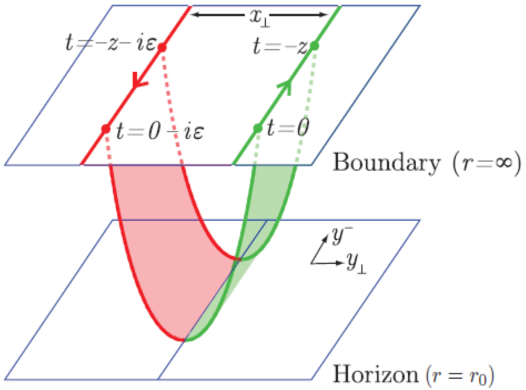

H. Liu, K. Rajagopal, and U. A. Wiedemann,
Phys. Rev. Lett. 97, 182301 (2006).

NL correction to jet quenching parameter

Zhang, Hou, Ren, JHEP1301 (2013) 032

dominant

$$\hat{q} = \frac{\pi^{3/2}\Gamma(\frac{3}{4})}{\Gamma(\frac{5}{4})}\sqrt{\lambda}T^3[1-\underline{1.97\lambda^{-1/2}}+O(\lambda^{-1})]$$

$$1 - \underline{1.765\lambda^{-3/2}}.$$

Armesto et al JHEP09 (06)

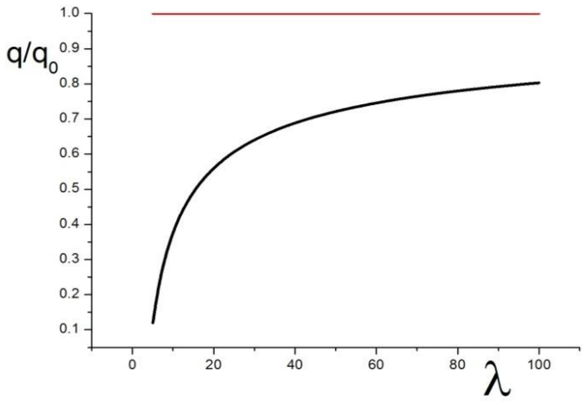

相变温度附近的喷注淬火参数

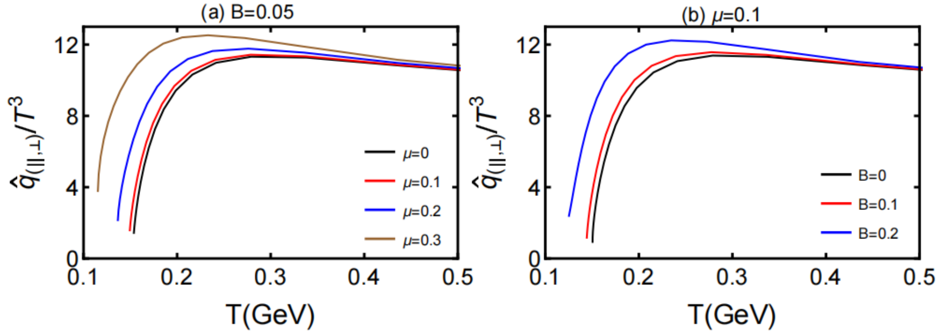

图10. $\hat{q}_{(\parallel,\perp)}$

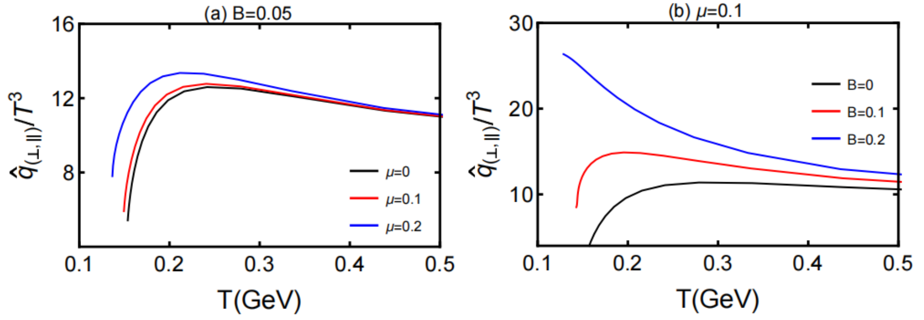

图11. $\hat{q}_{(\perp,\parallel)}$

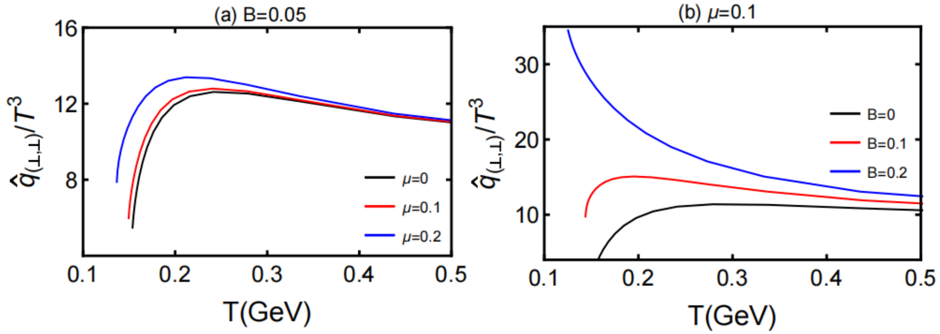

图12. $\hat{q}_{(\perp,\perp)}$

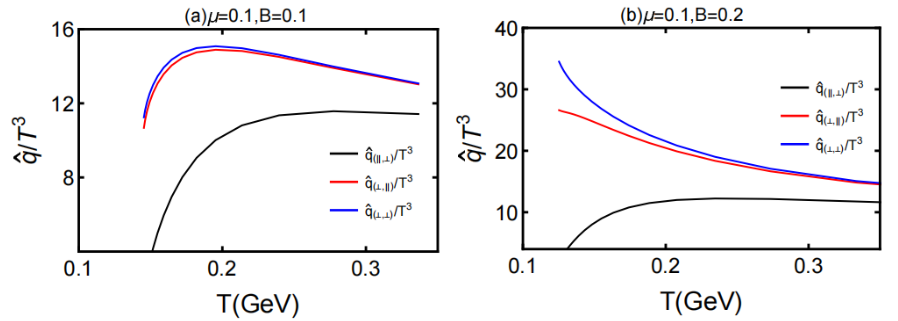

图13. $\hat{q}/T^3$

图10–12：$\hat{q}$在T_c附近有增强，与格点(150-250MeV)相符合*；峰值所对应温度随μ/B增加而降低；μ、B增强了$\hat{q}$

图13：$\hat{q}_{(\perp,\perp)} > \hat{q}_{(\perp,\parallel)} > \hat{q}_{(\parallel,\perp)} \longrightarrow \hat{q}_{\perp} > \hat{q}_{\parallel}$

Amit Kumar,Abhijit Majumder,and Johannes Heinrich Weber. PRD 106 (2022) 3, 034505

Zhou-Run Zhu, De-fu Hou, Inverse magnetic catalysis and energy loss in holographic QCD model, (arXiv:2305.12375). Appear in PRD (2004)

相变温度附近的重夸克能损

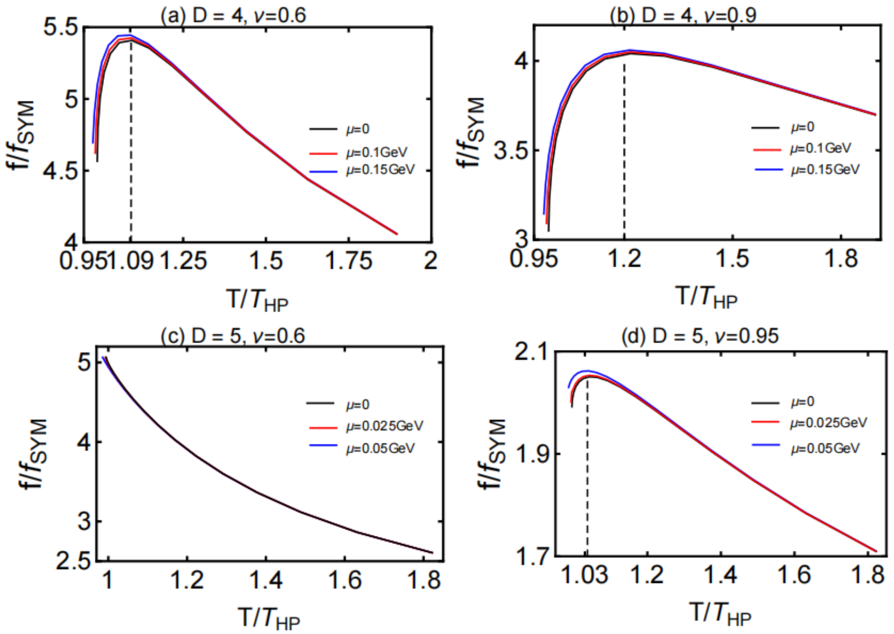

图24. 化学势的对能损的影响

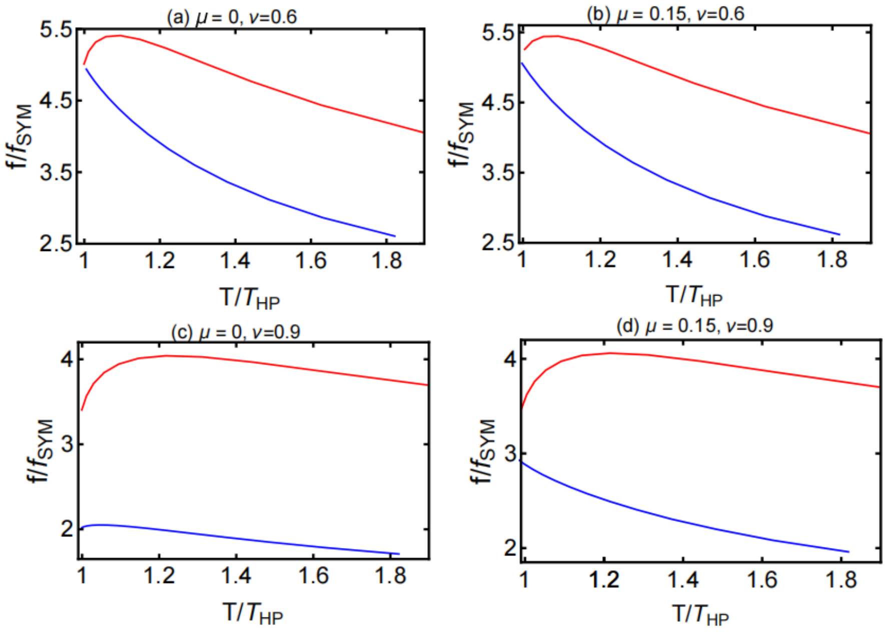

图25. 不同维度下的能损

1) 在T_c附近有增强，峰值所对应温度随μ增加而降低；
2)在较低维度时，重夸克损失更多能量。

Zhou-Run Zhu, Jun-Xia Chen, Xian-Ming Liu, De-fu Hou, Eur.Phys.J.C 82 (2022) 6,560.

Heavy quark potential $V_{\parallel}$

$$V(L) = V_0(L) + \omega^2 l_0^2 V_1(L) + O(\omega^4)$$

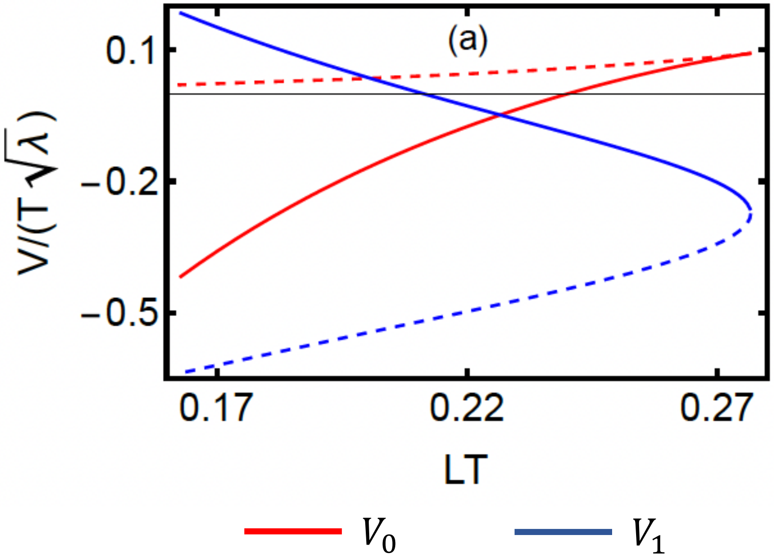

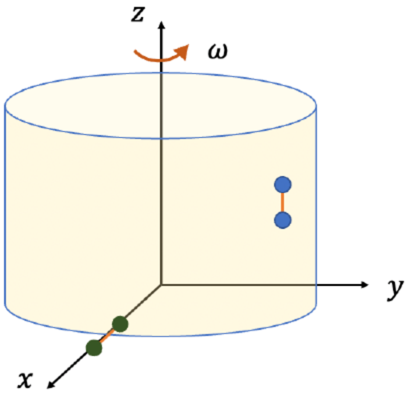

1. Binding force ↓
2. Force range ↑

$$\delta L = \frac{|V_1(L_0)|}{V_0'(L_0)} \omega^2 l_0^2 \qquad V_0(L_0) = 0$$

J.X. Chen, DH, H.C Ren , JHEP03 (2024) 171 , arXiv: 2308.08126

Heavy quark potential $V_{\perp}$

$$V(L) = V_0(L) + \frac{1}{4}\omega^2 L^2 V_1(L) + O(\omega^4)$$

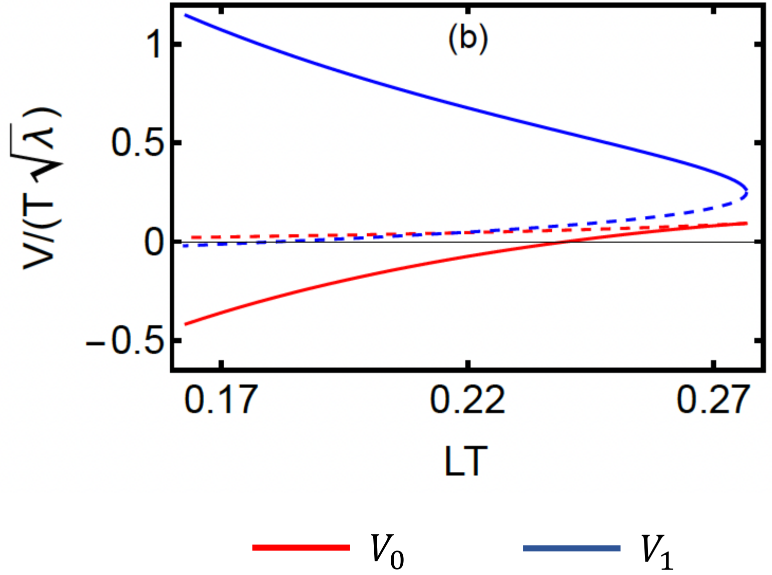

1. Potential
2. Force range

$$V_0(L_0) = 0$$

$$\delta L = -\frac{V_1(L_0)}{4V_0'(L_0)}\omega^2 L_0^2$$

Dragging force

J.X. Chen, DH, H.C Ren , JHEP03 (2024) 171 , arXiv: 2308.08126

Components of drag force

$$\frac{dp_\mu}{dt} = -\frac{1}{2\pi\alpha'}\frac{\partial\mathcal{L}}{\partial(\frac{\partial X^\mu}{\partial r})}$$

Drag force of μ component

Azimuthal $$\frac{dp_\phi}{dt} = -\frac{\pi\sqrt{\lambda}T^2}{2}\omega l_0^2\frac{1}{\sqrt{1-v^2}}$$

Radial $$\frac{dp_l}{dt} = -\omega^2 l_0\frac{1}{\sqrt{1-v^2}}\left[\frac{T\sqrt{\lambda}}{2(1-v^2)^{\frac{1}{4}}} - \boxed{m_{rest}}\right]$$

cut off $r_m = 2\pi\alpha' m_{rest}$

Longitudinal $$\frac{dp_z}{dt} = -\frac{\pi\sqrt{\lambda}T^2}{2}\frac{v}{\sqrt{1-v^2}}\left(1+\underline{\frac{\omega^2 l_0^2}{2}\frac{1}{1-v^2}}\right)$$

$\propto \omega^2$

$\boxed{\omega = 0}$ $\Rightarrow$ $$\frac{dp_\phi}{dt} = 0, \quad \frac{dp_l}{dt} = 0, \quad \frac{dp_z}{dt} = -\frac{\pi\sqrt{\lambda}T^2}{2}\frac{v}{\sqrt{1-v^2}}$$

S. S. Gubser, PRD74, 126005 (2006); C. P. Herzog, etc. JHEP 07, 013 (2006).

Holographic spin alignment of J/ψ meson in magnetized plasma

Y.-Q. Zhao, XLS, S.-W. Li, D. Hou,
arXiv:2403.07468 , accepted by JHEP

Dimuon production rate

- **S-matrix element($J/\psi \to \mu^+\mu^-$):**

  [4]. C. Gale and J. I. Kapusta, "Vector dominance model at finite temperature," Nucl. Phys. B 357 (1991) 65–89

$$S_{fi} = \int d^4x \int d^4y \left\langle f, \mu^+\mu^- \left| J_\alpha(y) G_R^{\alpha\beta}(x-y) J_\beta^l(x) \right| i \right\rangle$$

where

J_α is the current that couples to J/ψ;

J_β^l is the leptonic current

$$J_\beta^l(x) \equiv g_{M\mu^+\mu^-} \overline{\psi}_l(x) \Gamma_\beta \psi_l(x)$$

- **Retarded propagator (vacuum):**

$$G_R^{\alpha\beta}(p) = -\frac{\eta^{\alpha\beta} + p^\alpha p^\beta / p^2}{p^2 + m_{J/\psi}^2 + i m_{J/\psi} \Gamma}$$

- **Total dimuon production rate:**

$$\begin{aligned} N &= -2g_{M\mu^+\mu^-}^2 \int \frac{d^3\mathbf{p}_+}{(2\pi)^3 E_+} \frac{d^3\mathbf{p}_-}{(2\pi)^3 E_-} [G_R^{\rho\sigma}(p)]^* G_R^{\alpha\beta}(p) \\ &\quad \times n_B(\omega) \mathrm{Im} D_{\rho\alpha}(p) \left[p_\beta^- p_\sigma^+ + p_\beta^+ p_\sigma^- - g_{\beta\sigma}(p_+ \cdot p_- + m_\mu^2) \right] \end{aligned}$$

- **Differential production rate:**

$$\begin{aligned} \frac{dN}{d^4p \, d\cos\theta^* d\varphi^*} &= -\frac{g_{M\mu^+\mu^-}^2}{2(2\pi)^6} \sqrt{1 + \frac{4m_\mu^2}{p^2}} [G_R^{\rho\sigma}(p)]^* G_R^{\alpha\beta}(p) \\ &\quad \times n_B(\omega) \mathrm{Im} D_{\rho\alpha}(p) \left(p_\beta p_\sigma - 4 q_\beta q_\sigma - g_{\beta\sigma} p^2 \right) \end{aligned}$$

$$\begin{aligned} \frac{dN}{d^4p \, d\cos\theta^* d\varphi^*} &= \frac{3C_N}{8\pi} \left\{ \frac{p^2}{p^2 - 2m_\mu^2} - \frac{p^2 + 4m_\mu^2}{p^2 - 2m_\mu^2} \left[\frac{1 - \rho_{00}}{2} + \frac{3\rho_{00} - 1}{2} \cos^2\theta^* \right. \right. \\ &\quad - \mathrm{Re}\rho_{1,-1} \sin^2\theta^* \cos 2\varphi^* + \frac{\mathrm{Re}(\rho_{0,-1} - \rho_{01})}{\sqrt{2}} \sin 2\theta^* \cos\varphi^* \\ &\quad \left. \left. + \mathrm{Im}\rho_{1,-1} \sin^2\theta^* \sin 2\varphi^* - \frac{\mathrm{Im}(\rho_{0,-1} + \rho_{01})}{\sqrt{2}} \sin 2\theta^* \sin\varphi^* \right] \right\} \end{aligned}$$

- **Spin matrix:**

$$\boxed{\rho_{\lambda\lambda'}(p) \equiv -\frac{2g_{M\mu^+\mu^-}^2}{3(2\pi)^5 C_N} \left(1 - \frac{2m_\mu^2}{p^2} \right) \sqrt{1 + \frac{4m_\mu^2}{p^2}} \frac{p^2 n_B(\omega) \varrho_{\lambda\lambda'}}{(p^2 + m_{J/\psi}^2)^2 + m_{J/\psi}^2 \Gamma^2}}$$

Numerical results

- Magnetic field parallel to momentum

$\mathbf{p} = (0, 0, p)$ $T = 0.2\ \text{GeV}$

- Spectral Function:

$\boldsymbol{P = 0}$ $\boldsymbol{P = 5\ GeV}$ $\boldsymbol{P = 10\ GeV}$

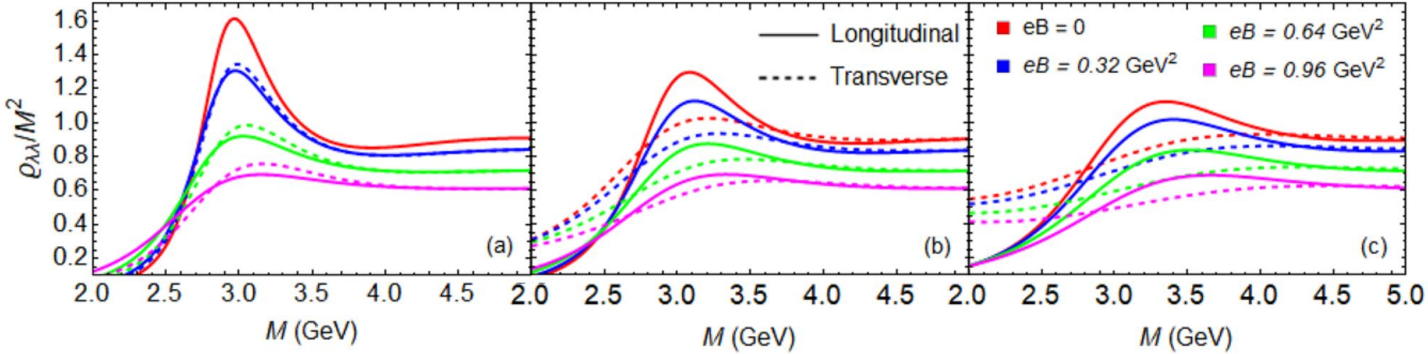

A nonzero magnetic field or a nonzero momentum will induce a separation between longitudinally and transversely polarized modes.

Numerical results

- Magnetic field parallel to momentum

$$\mathbf{p} = (0,0,p) \quad T = 0.2\ \text{GeV}$$

- Spin alignment:

$$\lambda_\theta = \frac{1-3\rho_{00}}{1+\rho_{00}},$$

[5]. Z.-T. Liang, X.-N. Wang, Spin alignment of vector mesons in non-central A+A collisions, Phys. Lett. B 629 (2005) 20–26.

High T→monotonic ;

Low T → non-monotonic.

Magnetic Field:

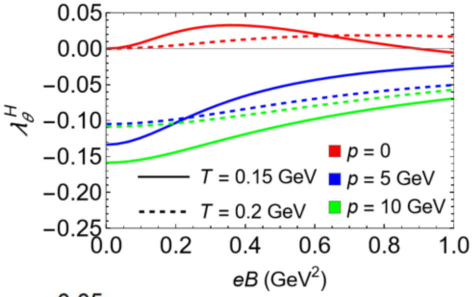

Momentum:

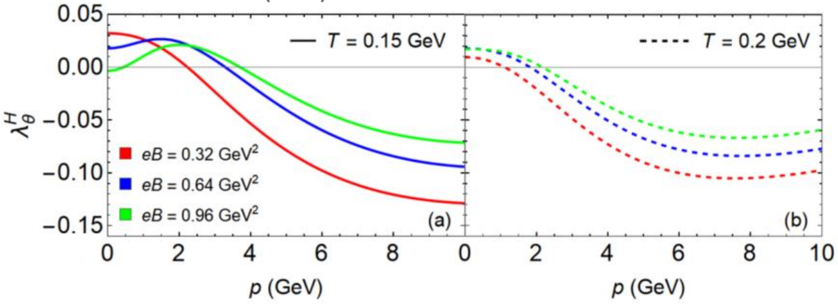

- **Application to heavy-ion collisions(the direction of magnetic field along the y-direction)**

- **Spin alignment:**

$$\boxed{T = 0.15\ \mathrm{GeV}}$$

$$\boxed{\mathbf{p} = \left(p_T\cos\varphi, p_T\sin\varphi, \sqrt{M^2+p_T^2}\sinh(Y)\right)}$$

$$\lambda_\theta = \frac{1-3\rho_{00}}{1+\rho_{00}},$$

$$\lambda_\varphi = \frac{2\mathrm{Re}\rho_{1,-1}}{1+\rho_{00}},$$

$$\lambda_{\theta\varphi} = \frac{\sqrt{2}\mathrm{Re}(\rho_{01}-\rho_{0,-1})}{1+\rho_{00}},$$

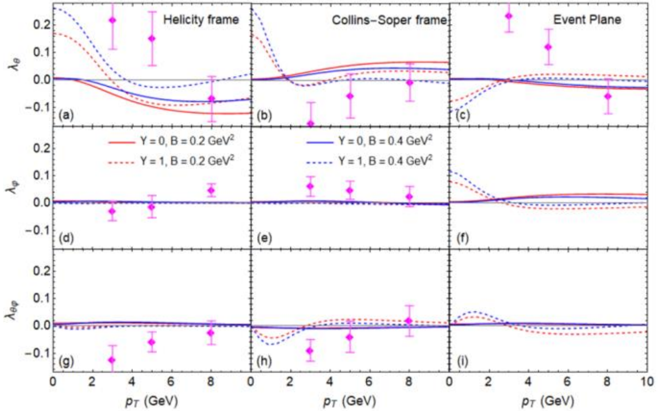

[6]. ALICE Collaboration, "Measurement of the J/ψ Polarization with Respect to the Event Plane in Pb-Pb Collisions at the LHC," PRL 131 no. 4, (2023) 042303

Y.-Q. Zhao, XLS, S.-W. Li, D. Hou, arXiv:2403.07468 , accepted by JHEP

For the helicity frame and the Collins-Soper frame, we find that the λ_θ parameter is dominant when measuring along the event plane direction, all three parameters $\lambda_\theta^{\mathrm{EP}}$, $\lambda_\varphi^{\mathrm{EP}}$, and $\lambda_{\theta\varphi}^{\mathrm{EP}}$ are of the same order.

Summary outlook

Properties of strongly interacting matter under extreme conditions are very interesting!

- **QCD Phase diagram under magnetic field & rotation (IMC)**
- **Jet quenching and energy loss**
- **Heavy quark potential and dragging force**
- **Spectral function and and spin alignment**
- **How to understand the different results of rotation from lattice？**

（Polarization induced by Magnetic field and rotation?

Summary

- Lect1: Brief introduction to QFT at Finite T and density
  HT(D)Ls , DSE, Renormalization

- Lect2. Dense QCD matter (CSC, FRGE)

- Lect3. Transports

- Lect4. Holographic study of sQCD matter under extreme conditions

Outlook

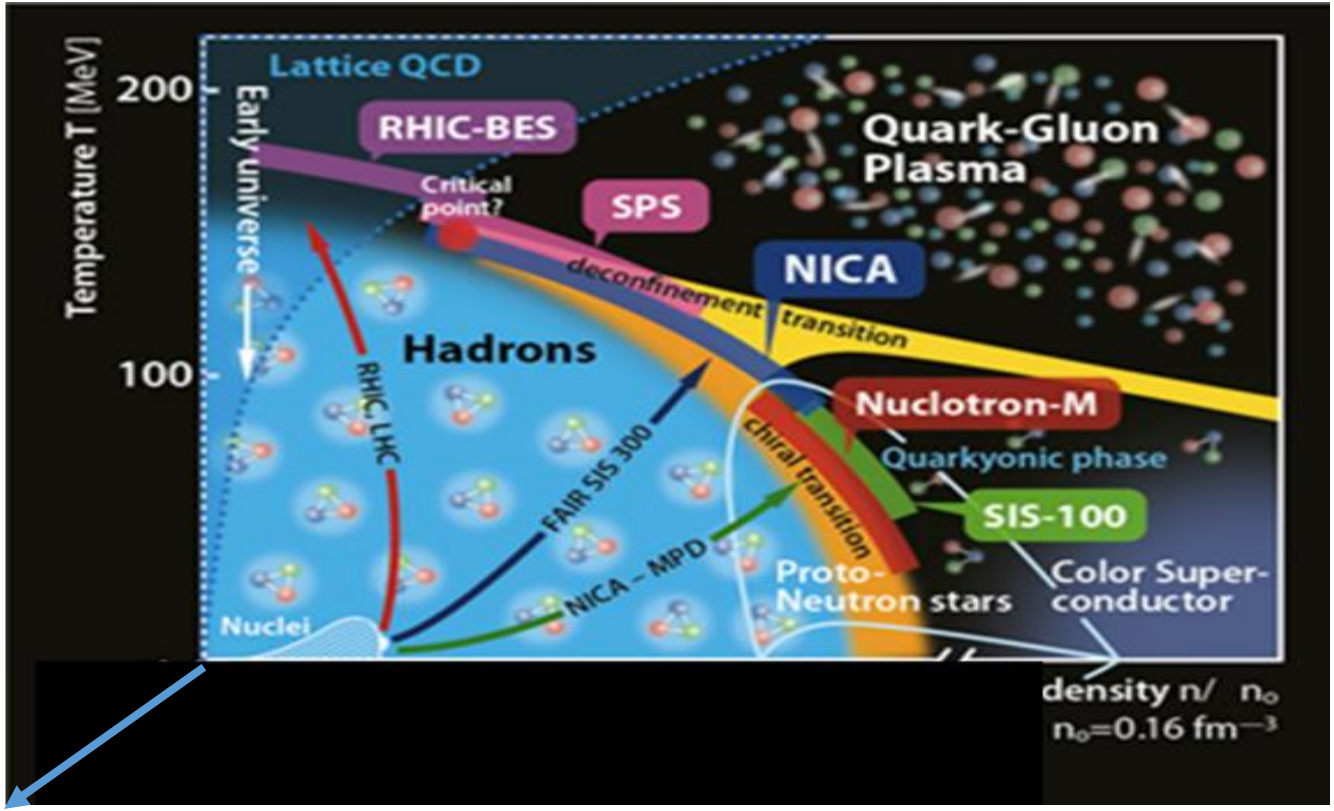

B, ω, ni

构造致密QCD物质的状态方程

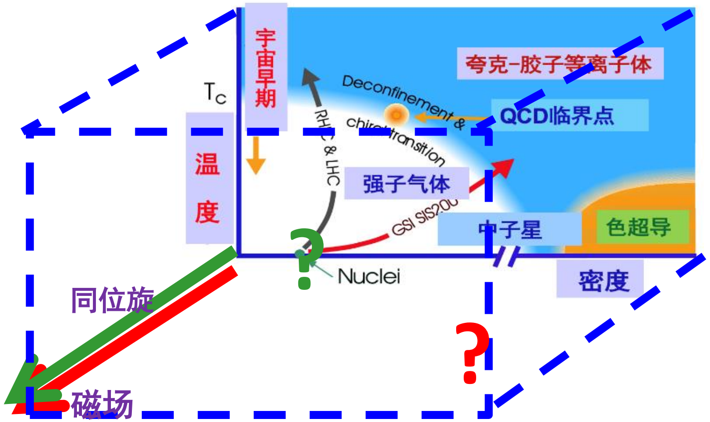

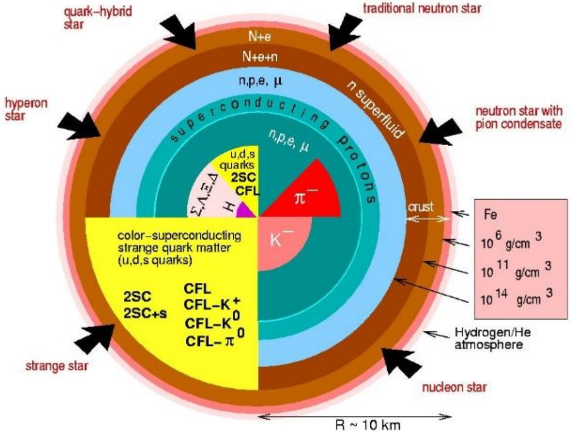

- **状态方程**：是重离子碰撞流体动力学模拟的关键输入量；
  影响致密天体质量半径关系
- **关键问题**：随着寻找QCD临界点的束流能量扫描实验向低能高密推进，
  流体动力学演化需要高密区QCD物质的状态方程

2. 计算致密 QCD 物质输运系数

- **输运系数**：剪切粘滞、体粘滞、电导率、扩散系数
- **计算目标**：理论计算致密QCD物质输运系数对温度、重子化学势以及其它守恒荷化学势的依赖
- **科学难题**：在非零重子化学势区域，第一性原理 Lattice QCD 计算遭遇“符号问题”困难。
- **理论方法**：温度场论、引力场论对偶、泛函重整化群
- **应用场景**：作为粘滞流体力学数值算法的输入，模拟核核碰撞

重离子碰撞和中子星并合的演化→ 必须研究致密QCD物质输运系数！

De Hass-van Alphen Effect with Rotation

Shu-Yun Yang, Ren-Da Dong, DF Hou, Hai-Cang Ren, PRD 107, 076020 (2023)

finite T

$$P_{\mathrm{dHvA}} = -\frac{(eB)^{\frac{1}{2}}}{2\pi^2 R^2} \sum_{l=1}^{\infty} \frac{1}{l^{3/2}} \sum_{M>0} \frac{\cos\left[\frac{l\pi}{eB}(\mu + M\omega)^2 - \frac{\pi}{4}\right]}{\sinh \frac{2l\pi^2 T(\mu+M\omega)}{eB}}.$$

Zero T:

$$P_{\mathrm{dHvA}} = -\frac{(eB)^{\frac{3}{2}}}{4\pi^4 R^2} \sum_{M>0} \frac{1}{\mu + M\omega} \sum_{l=1}^{\infty} \frac{1}{l^{5/2}} \cos\left[\frac{l\pi}{eB}(\mu + M\omega)^2 - \frac{\pi}{4}\right]$$

In rotation, the thermodyn Equl. is established under a AM. The equal distrib. of different AM states within a LL is offset by the nonzero AV with higher AM more favored than lower ones, which amounts to lifting the degeneracy of LL. The dHvA oscillation is thereby expected to be reduced by rotation

De Hass-van Alphen Effect with Rotation

dHvA in NS with rotation (R=1km)

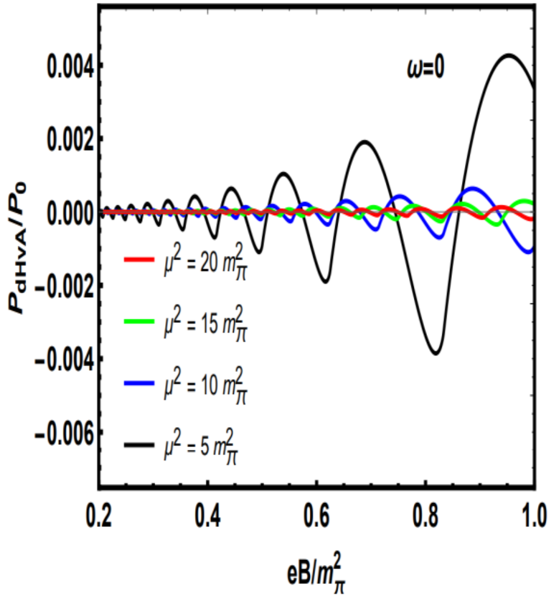

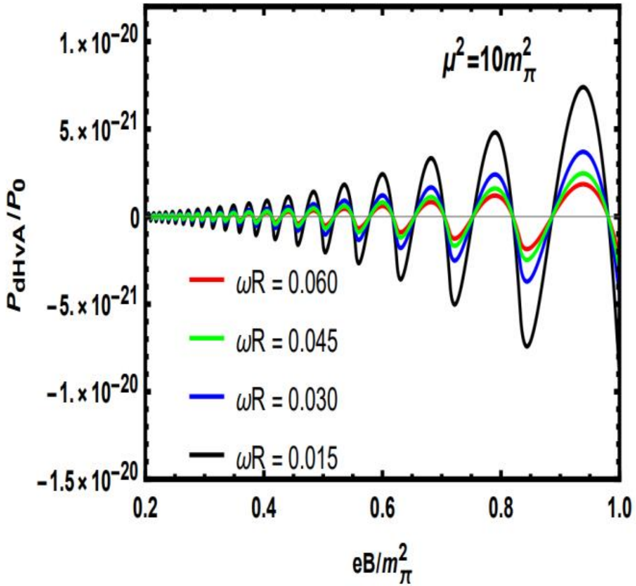

Huge suppression of dHvA oscill.(17 order)
due to large size

Shu-Yun Yang, Ren-Da Dong, DF Hou, Hai-Cang Ren, PRD 107, 076020 (2023)